

Contribution from the Department of Chemistry and Materials Science Center, Cornell University, Ithaca, New York 14853-1301

Bonding in Halocuprates

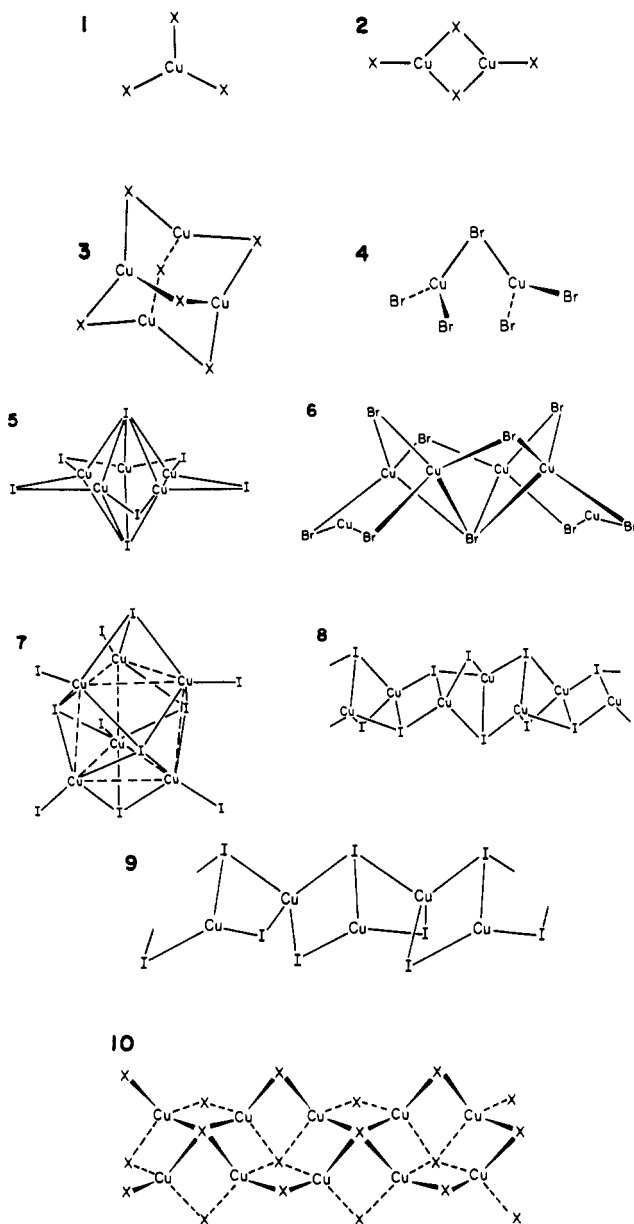
Lalitha Subramanian and Roald Hoffmann*

Received June 16, 1991

The unusual square pyramidal geometry around halogen atoms bridging four Cu atoms in halocuprates is studied within the extended Hückel framework. Calculations are performed on the discrete molecular anion $[\text{Cu}_6\text{Br}_9]^{3-}$, as well as on the one-dimensional polymeric $[\text{Cu}_2\text{Br}_3]^-$ structure. We examine the bonding between the bridging Br and Cu atoms in planar and nonplanar model systems. Br should be capable of bridging as many as six Cu atoms. In the higher coordinations pyramidal geometry is favored; the bonding is perforce delocalized, an extension of three-center bonding. A few hypothetical structures of halocuprates with a tetrahedral and a square pyramidal $\mu_4\text{-X}$ are predicted.

Halocuprate Geometries

There is wide variety in the structures of copper(I) halocuprates, $\text{Cu}_x\text{X}_y^{n-}$. These molecules may form discrete geometries of varying nuclearity or polymeric extended systems. The halogens range from terminally bonded to bridging no less than five metals in the discrete structures, while in polymeric systems they bridge two, three, or four metal atoms. Structures 1-10 show some of the geometries observed.



Molecules 1-4 are discrete anions with halogen atoms in terminal and doubly bridging position, while in 5 the halides bridge

two and five coppers. 6 is a $\text{Cu}_6\text{Br}_9^{3-}$ system where Br bridges two and four Cu atoms; in 7 there is an unusual capped prismatic structure. 8 is a polymeric iodocuprate where I bridges two and three Cu atoms, while the geometry around Cu is approximately tetrahedral. 9 is another polymer with Cu exhibiting distorted trigonal and tetrahedral geometries. In 10, we see an extended halocuprate where the halogens bridge two and four metal atoms with the geometry around the metal atom being tetrahedral. The $\mu_4\text{-X}$ is at the apex of a square pyramid, as it is in the discrete molecule 6. Table I lists some structural parameters of a selection of halocuprates known.

This fantastic structural richness is exhibited almost without exception in the context of salts consisting of molecular or polymeric $\text{Cu}_x\text{X}_y^{n-}$ anions and various, often organic counteranions. A series of systematic studies on halocuprates indicates that the anionic configuration, i.e., the coordination number of Cu(I) and the tendency of the anion to form extended structures, depends on the degree of dilution imposed on the ligands by the cation.¹ Bulky cations which have low well-screened charges favor the formation of discrete anions in which Cu(I) has a low coordination number. Small cations, in contrast, favor the formation of extended structures, where Cu(I) shows a higher coordination number of 4. A similar trend is observed for the haloargentates as well.²⁻⁶

With an increase in the bulkiness of the metal or halogen used, the tendency of the anion toward polymerization increases, and the metal atom prefers four-coordination. Early work by Romming and Waerstad⁷ showed that the intermediate in the Sandmeyer reaction consists of polymeric anion chains. Another system reported by Boehm et al.⁸ is $[(\text{CH}_3)_2\text{N}_2\text{CHN}_2(\text{CH}_3)_2][\text{Cu}_2\text{Br}_3]$

- (1) Andersson, S.; Jagner, S. *Acta Chem. Scand.*, A 1989, 43, 39.
- (2) (a) Jagner, S.; Olson, S.; Stomberg, R. *Acta Chem. Scand.*, A 1986, 40, 230. (b) Helgesson, G.; Jagner, S. *J. Chem. Soc., Dalton Trans.* 1988, 2117. (c) Helgesson, G.; Jagner, S. *J. Chem. Soc., Dalton Trans.* 1990, 2413. (d) Andersson, S.; Helgesson, G.; Jagner, S.; Olson S. *Acta Chem. Scand.*, A 1989, 43, 946. (e) Jagner, S.; Helgesson, G. *Adv. Inorg. Chem.*, in press.
- (3) Gilmore, C. J.; Tucker, P. A.; Woodward, P. *J. Chem. Soc. A* 1971, 1337.
- (4) Meyer, H. J. *Acta Crystallogr.* 1963, 16, 788.
- (5) Peters, K.; von Schering, H. G.; Ott, W.; Seidenspinner, H.-M. *Acta Crystallogr.*, C 1984, 40, 789.
- (6) Brink, C.; Stenfort Kroese, H. A. *Acta Crystallogr.* 1952, 5, 433.
- (7) Romming, Chr.; Waerstad, K. *Chem. Commun.* 1965, 299.
- (8) Boehm, J. R.; Balch, A. L.; Bizot, K. F.; Enemark, J. H. *J. Am. Chem. Soc.* 1975, 97, 501.
- (9) Asplund, M.; Nilsson, M.; Jagner, S. *Acta Chem. Scand.*, A 1983, 37, 57.
- (10) Asplund, M.; Nilsson, M.; Jagner, S. *Acta Chem. Scand.*, A 1984, 38, 57.
- (11) Andersson, S.; Jagner, S. *Acta Chem. Scand.*, A 1986, 40, 52.
- (12) Andersson, S.; Jagner, S.; *Acta Chem. Scand.*, A 1985, 39, 799.
- (13) Andersson, S.; Jagner, S. *Acta Chem. Scand.*, A 1985, 39, 515.
- (14) Andersson, S.; Jagner, S. *Acta Chem. Scand.*, A 1985, 39, 577.
- (15) Andersson, S.; Jagner, S. *Acta Chem. Scand.*, A 1985, 39, 297.
- (16) Asplund, M.; Jagner, S. *Acta Chem. Scand.*, A 1984, 38, 135.
- (17) Andersson, S.; Jagner, S. *Acta Chem. Scand.*, A 1985, 39, 423.
- (18) Andersson, S.; Jagner, S. *Acta Chem. Scand.*, A 1987, 41, 230.
- (19) Asplund, M.; Jagner, S. *Acta Chem. Scand.* A 1984, 38, 255.
- (20) Andersson, S.; Jagner, S. *Acta Crystallogr.*, C 1987, 43, 1089.
- (21) Asplund, M.; Jagner, S. *Acta Chem. Scand.*, A 1984, 38, 411.
- (22) Asplund, M.; Jagner, S.; Nilsson, M. *Acta Chem. Scand.*, A 1982, 36, 751.

Table I. Selected Halocuprate Structures

compound		coord no. of Cu(I)	Cu-X, \AA	Cu...Cu, \AA	structural type	ref
cation	anion					
NBu ₄ ^a	CuCl ₂	2	2.107		discrete linear	9
NBu ₄	CuBr ₂	2	2.227		discrete linear	9
NBu ₄	CuBrCl	2	2.195, 2.104		discrete linear	10
NPr ₄ ^b	CuCl ₂	2	2.071		discrete linear	11
NPhMe ₃ ^c	CuCl ₂	2	2.117		discrete linear	12
PPh ₃ Et ^d	CuBr ₂	2	2.224		discrete linear	13
PPh ₃ Pr	CuBr ₂	2	2.225		discrete linear	14
AsPh ₄	CuCl ₂	2	2.072		discrete linear	15
PPh ₄	CuCl ₂	2	2.080		discrete linear	16
PPh ₄	CuBr ₂	2	2.211		discrete linear	16
NEt ₄	Cu ₂ Br ₄	3	2.319, 2.441	2.937	2 ^f	16
NPhMe ₃	Cu ₂ Br ₄	3	2.310, 2.421	2.738	2	17
PMe ₄	CuBr ₃	3	2.365		1	18
PEt ₄	Cu ₂ Br ₄	3	2.263, 2.423	2.870	2	19
PMePh ₃	Cu ₂ Br ₄	3	2.337, 2.426	2.697	2	20
NPr ₄	Cu ₂ I ₄	3	2.499, 2.571	2.698	2	21
NBu ₄	Cu ₂ I ₄	3	2.514, 2.566	2.726	2	22
PMePh ₃	CuI ₃	3	2.537		1	23
AsPh ₄	Cu ₂ I ₄	3	2.490, 2.578	2.663	2	24
NPr ₄	Cu ₄ Br ₆	3	2.373	2.718	3	25
PBuPh ₃	Cu ₄ Br ₆	3	2.410	2.719	3	26
PMePh ₃	Cu ₄ I ₆	3	2.638	2.742	3	27
NMe ₄	Cu ₂ Br ₅	3	2.381, 2.392	2.837	4	28
NMeBu ₃	Cu ₃ Br ₇	4	2.345, 2.912	2.605	5 ^g	29
NPr ₄	Cu ₃ I ₇	4	2.510, 2.640	2.580	5	30
NMeEt ₃	Cu ₆ Br ₉	2, 4	2.285, 2.697	3.030	6	1
NEt ₄	[Cu ₆ I ₁₁]I	4	2.567, 2.731	2.961	7	31
NMe ₄	Cu ₂ I ₃	4	2.517	2.452	polymeric chain 8	32
NMe ₄	Cu ₂ Cl ₃	4	2.254, 2.494	2.869	polymeric chain 10	33
(Me ₂ N ₂) ₂ CH	Cu ₂ Br ₃	4	2.431, 2.600	3.03	polymeric chain 10	8
SMe ₃	Cu ₂ I ₃	4	2.612, 2.724	2.954	polymeric chain 10	34
NEt ₄	Ag ₂ Cl ₃	4	2.519, 2.679	3.348	polymeric chain 10	35
NMe ₄	Ag ₂ Br ₃	4	2.612, 2.804	3.078	polymeric chain 10	35
S ₂ C ₃ (SCH ₃) ₃	Cu ₂ I ₃	3, 4	2.523, 2.730	2.551	polymeric chain 9	36
C ₂₃ H ₁₇ S	Cu ₂ I ₃	4	2.651, 2.542	2.479	polymeric chain ^h	37

^aTetra-*n*-butyl. ^bPropyl. ^cPhenyl. ^dEthyl. ^eOnly the shortest distance is quoted. ^fNumbers refer to the text structures. ^gIn the bromide structure the halides are not coplanar with the coppers. ^hThis structure resembles chain 8.

wherein the anion has an extended structure. Since then several other polymeric systems have been made.

While we would love to understand in detail why a given cation leads to a specific counteranion aggregation mode of Cu⁺ and X⁻ entities, we cannot be optimistic about theory contributing decisively to an answer of that basic chemical question. The thermodynamics of aggregation is not easy to predict, especially in structures partly covalent and partly ionic, and the aggregation forces may be under kinetic control. The more restricted aim of this paper is to examine the peculiar bonding modes of the halides, in particular the strange μ_4 square pyramidal and μ_5 configurations. It is easy to understand, in the context of normal ideas about coordinate covalent bonding, the nature of terminal, μ_2 , μ_3 , and tetrahedral μ_4 halides. But the nontetrahedral μ_4 and the μ_5 systems are at first sight strange.

A word about the copper-halogen bond metrics is in order. The Cu-X bond distances listed in Table I indicate that as the extent of bridging around the halogen atom increases, the bond distances also increase. The Cu-Cl distances vary from 2.107 to 2.254 and 2.494 \AA as the Cl goes from terminal to bridging two and four Cu atoms. The Cu-Br distance increases from 2.227 \AA to 2.421, 2.600, and 2.912 \AA as the Br goes from terminal to bridging two, four, and five Cu atoms, respectively. The Cu-I distance changes from 2.499 to 2.571, 2.517, 2.724, and 2.640 \AA as the I goes from terminal to bridging two, three, four, and five Cu atoms. Except for the μ_3 -I and the μ_5 -I cases, there seems to be a general tendency for the Cu-X distance to increase with bridging.

We begin our study with the bonding of nontetrahedral μ_4 -Br compounds, 6 and 10. In both these systems, the μ_4 -Br atom occupies the apex of a square pyramid formed by four Br-Cu bonds with a tetrahedral geometry around each Cu atom. We have performed the relevant calculation using extended Hückel method,³⁸⁻⁴³ the parameters are listed in the Appendix.

In the polymeric Cu₂Br₃⁻ system,⁸ the anions are well-separated from the organic cation. As can be seen in 10, the μ_4 -Br atoms are alternately above and below the plane of the Cu atoms. The μ_2 -Br atoms also alternate with the μ_4 -Br atoms. The μ_4 -Br-Cu distance varies from 2.58 to 2.609 \AA while μ_2 -Br-Cu is 2.432 \AA .

The μ_4 -Br-Cu distance in the extended structure 10 is approximately 0.1 \AA shorter than that reported for the discrete

- (23) Bowmaker, G. A.; Clark, G. R.; Rogers, D. A.; Camus, A.; Marsich, N. *J. Chem. Soc., Dalton Trans.* **1984**, 37.
 (24) Asplund, M.; Jagner, S. *Acta Chem. Scand.*, **A 1984**, 38, 297.
 (25) Asplund, M.; Jagner, S. *Acta Chem. Scand.*, **A 1984**, 38, 725.
 (26) Andersson, S.; Jagner, S. *Acta Chem. Scand.*, **A 1986**, 40, 210.
 (27) Bowmaker, G. A.; Clark, G. R.; Yuen, D. K. P. *J. Chem. Soc., Dalton Trans.* **1976**, 2329.
 (28) Asplund, M.; Jagner, S. *Acta Chem. Scand.*, **A 1985**, 39, 47.
 (29) Andersson, S.; Jagner, S. *J. Crystallogr. Spectrosc. Res.* **1988**, 18, 591.
 (30) Hartl, H.; Mahdjour-Hassan-Abadi, F. *Angew. Chem., Int. Ed. Engl.* **1984**, 23, 378.
 (31) Mahdjour-Hassan-Abadi, F.; Hartl, H.; Fuchs, J. *Angew. Chem., Int. Ed. Engl.* **1984**, 23, 514.
 (32) Andersson, S.; Jagner, S. *Acta Chem. Scand.*, **A 1985**, 39, 181.
 (33) Andersson, S.; Jagner, S. *Acta Chem. Scand.*, **A 1986**, 40, 177.
 (34) Andersson, S.; Jagner, S.; Nilsson, M. *Acta Chem. Scand.*, **A 1985**, 39, 447.
 (35) Helgesson, G.; Jagner, S. *Acta Crystallogr.*, **C 1988**, 44, 2059.
 (36) Asplund, M.; Jagner, S. *Acta Chem. Scand.*, **A 1984**, 38, 129.
 (37) Batsanov, A. S.; Struchkov, Yu. T.; Ukhin, L. Yu.; Dolgoplova, N. A. *Inorg. Chim. Acta* **1982**, 63, 17.

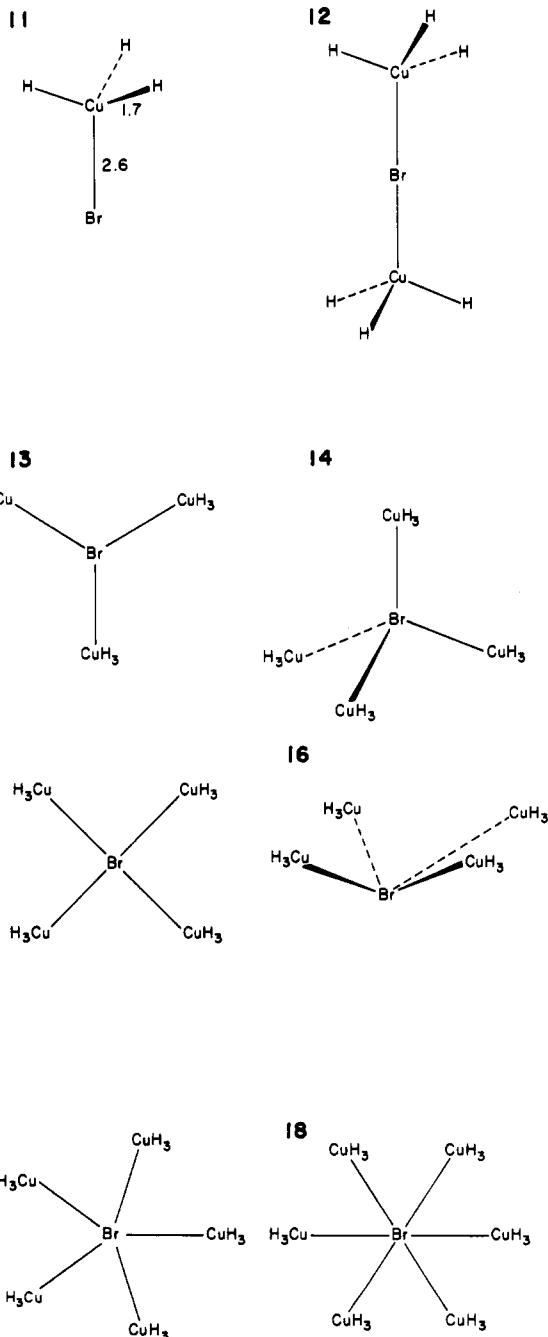
- (38) Hoffmann, R. *Solids and Surfaces: A Chemist's View of Bonding in Extended Structures*; VCH: New York, 1988.
 (39) Hoffmann, R. *Angew. Chem., Int. Ed. Engl.* **1987**, 26, 846.
 (40) Hughbanks, T.; Hoffmann, R. *J. Am. Chem. Soc.* **1983**, 105, 1150.
 (41) Hoffmann, R.; Whangbo, M.-H. *J. Am. Chem. Soc.* **1978**, 100, 6093.
 (42) Whangbo, M.-H.; Hoffmann, R.; Woodward, R. B. *Proc. R. Soc. London*, **A 1979**, 366, 23.
 (43) Hoffmann, R. *Rev. Mod. Phys.* **1988**, 60, 601.

molecule $[N(Me)(Et)_3]_3[Cu_6Br_9]$. In the discrete molecule, the Cu...Cu distance along the a -axis is 3.199 Å and that along the c -axis is 2.862 Å. In both, the discrete molecule and the polymeric system, the Cu...Cu distance is large compared to that in the metal, which is 2.55 Å.

Bonding in Model Bromocuprates

Our aim is 2-fold: (i) to understand the change in the Br-Cu bond lengths with variation in the number of atoms bridged by Br atom and (ii) to study the electronic structure and bonding in the unusual square pyramidal geometry around the μ_4 -Br.

To accomplish this, we have constructed model systems in which one Br atom is connected to varying number of Cu atoms, as shown in 11-18.



Structures 11-13, 15, 17, and 18 are models for μ_1 - μ_6 -Br coordination, idealized for the moment to in-plane bonding for μ_3 - μ_6 . 14 and 16 are alternative tetrahedral and square pyramidal μ_4 geometries, respectively. In each case the geometry around the Cu atoms is maintained as tetrahedral, three hydrogens completing the coordination sphere of each Cu. Consistent with a +1 oxidation state for Cu and -1 for H, each CuH_3 group enters

Table II. Reduced Overlap Population of Br-Cu and Cu...Cu Bonds for the Various Models

type	overlap population			Cu...Cu dist, Å
	Br-Cu (one bond)	Br-Cu (sum over all bonds)	Cu...Cu	
μ_1 -(11 ^a)	0.239	0.239		5.200
μ_2 -(12)	0.217	0.434	0.000	4.503
μ_3 -(13)	0.235	0.705	-0.001	4.246
tetr μ_4 -(14)	0.243	0.972	-0.001	3.677
plan μ_4 -(15)	0.218	0.872	-0.003	3.000
pyr μ_4 -(16)	0.219	0.876	-0.004	3.056
μ_5 -(17)	0.202	1.010	-0.031	2.600
μ_6 -(18)	0.177	1.062	-0.015	

^a Numbers refer to structures in the text.

the calculation with a 2- charge. In all the cases the Br-Cu distance has been maintained at 2.6 Å while the Cu-H distances were set at 1.7 Å. Note that we have kept the Br-Cu distance constant, knowing full well that in the real compounds it varies, increasing with the number of bonded Cu atoms. The philosophy of the approach is clear; i.e., we give the Cu-Br bond a chance to be equal in strength by making it of the same bond length in various geometries and then let the molecule tell us itself, through the overlap populations, what bond strength it desires. Table II shows the total and individual overlap population for the Cu-Br and the Cu...Cu bonds as well as the Cu...Cu distance for all the cases 11-18.

Thinking classically about these structures, we can consider the μ_1 , μ_2 , μ_3 , and tetrahedral μ_4 coordinations of Br as "normal" and the square pyramidal μ_4 , μ_5 , and μ_6 as untypical. Indeed the overlap populations in the first normal group are larger, consistently so, than in the second group. The exception is the linear μ_2 geometry. We could try a further analysis, using our prejudices about hybridization and the notion that an sp^3 - sp^3 bond should be weaker than an sp^3 - sp^2 or sp^3 - sp bond. The hybridization at Br in 11 is ambiguous (is it sp^3 or sp^2 ?), but for 12, most everyone would pick sp at Br, and for 13 sp^2 and for 14 sp^3 . In fact the Cu-Br overlap population rises along the series 12 → 13 → 14, instead of falling. The classical hybridization argument for bond strength does not work for bridging Br. This is confirmed by the Cu-X distances in Table I.

Hybridization is, of course, a qualitative valence bond notion, one of extreme heuristic value. The computed 4s and 4p orbital populations at Br in 12-14 do not match the expectations of sp , sp^2 , and sp^3 taken seriously, (i.e., 50%, 33%, and 25% s character, respectively), but the 4p orbital population does increase along this series.

It is interesting that the strongest Cu-Br bond is obtained for four Cu atoms tetrahedrally disposed around a Br. But there has been no report of a discrete bromocuprate where the geometry around a four-coordinate Br atom is tetrahedral! However, considering the solid-state cuprous halides,⁴⁴ CuCl, CuBr, and CuI crystallize in the zinc blende structure. At high temperatures, they transform to the wurtzite structure. In both these forms, the halogen atom has a tetrahedral environment. The argentous halides, AgF, AgCl, and AgBr, on the other hand, adopt the NaCl structure.⁴⁴ AgI prefers the wurtzite structure under normal conditions of temperature and pressure.⁴⁴ As for the aurous halides, structural information is available only for AuI, which consists of bent chains made up of alternating Au and I atoms.⁴⁵ The geometry around Au is linear while the Au-I-Au angle is 72°.

Returning to the halocuprate systems, the geometries 11-18 are idealized. In the real molecules where Br bridges two Cu atoms, μ_2 coordination is almost never linear and the μ_4 cases consistently pyramidal. This suggested a study of departures from linearity or planarity for the μ_2 - μ_6 structures. Figure 1a shows

(44) Lawn, B. R. *Acta Crystallogr.* **1964**, *17*, 1341. Burley, G. J. *Phys. Chem.* **1964**, *68*, 1111.

(45) Jagodzinski, H. Z. *Kristallogr.* **1959**, *112*, 80.

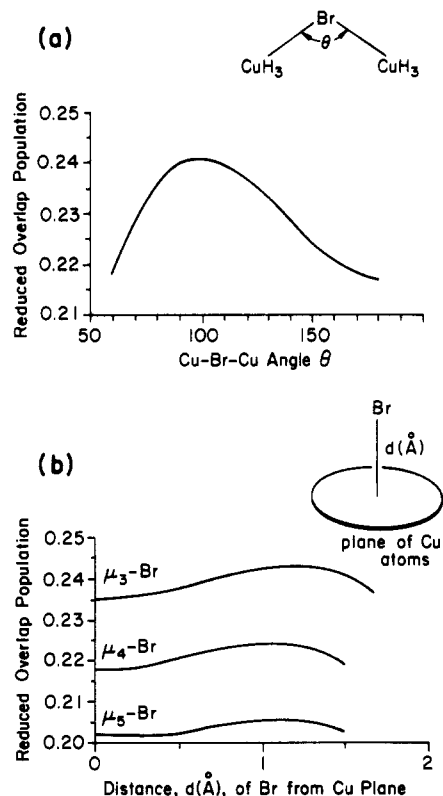


Figure 1. (a) Reduced overlap population as a function of Cu-Br-Cu angle, θ , for $\text{Br}(\text{CuH}_3)_2$ system. (b) Reduced overlap population as a function of distance of Br atom from the plane of Cu atoms for the three cases of Br bridging three, four, and five Cu atoms in $\text{Br}(\text{CuH}_3)_n$.

a plot of the overlap population of the Cu-Br bond as a function of the bridging angle, Cu-Br-Cu, for the case of Br bridging two Cu atoms.

There is maximum overlap population at an angle of 100° . A maximum is also seen in Figure 1b, which shows overlap population as a function of distance of Br from the plane of Cu atoms for the cases of Br bridging three, four and five Cu atoms. The Cu-Br bond length is maintained constant while the Br atom is pulled out of the plane of the Cu atoms. The overlap population decreases as we go from μ_3 to μ_4 to μ_5 -Br. With Br pulled out of the plane of the Cu atoms, the reduced overlap population first increases till the distance of 1.15 Å and then decreases for all three cases. The total energy varies little with the angle (or distance) for the μ_2 (or μ_5) case. For Br bridging two Cu atoms the energy minimizes at a Cu-Br-Cu angle of 100° . For the cases μ_3 - μ_5 , an energy minimum is obtained when the distance of Br atom from the plane of Cu atoms is 1.1 Å, which is also the distance at which the reduced overlap population is maximum.

Since it is possible that the total energy increases because the H atoms attached to the different Cu atoms come too close as the Cu-Br-Cu angle is decreased or as the distance of Br from the plane increases, we decided to repeat the calculations in the absence of H atoms. Similar results were obtained, with overlap population maxima and energy minima in some cases for a somewhat more out-of-plane Br-Cu_n geometry.

On the basis of these calculations, we may predict structural preferences for Br bridging different number of Cu atoms. For μ_2 -Br, a bent geometry is preferred over a linear one. For the cases of Br bridging three, four, and five atoms, pyramidal structures are more likely than planar geometries.

Though we have used the same bond length for Cu-Br, we get different overlap populations when Br bridges different number of Cu atoms, depending on the orientation of the Cu atoms around Br.

The question remains: Why does one see a high coordination number such as 5 for Br, as well as the unusual pyramidal μ_4 -Br coordination mode? In Table II we list another bond indicator, the sum of all Cu-Br overlap populations. This increases steadily

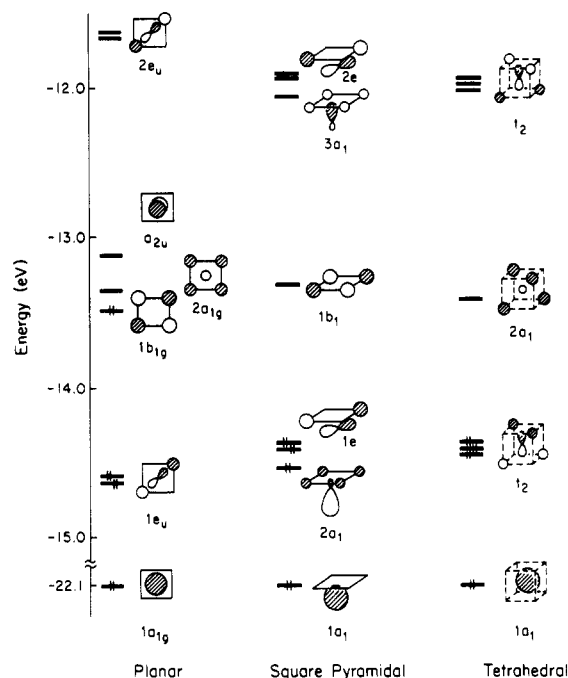


Figure 2. Molecular orbitals for planar, square pyramidal, and tetrahedral BrH_4^{3+} .

from μ_1 to μ_6 . While it seems to saturate, that limit is reached only at μ_6 . Obviously, Br is capable of forming more than four effective bonds. We proceed to a more detailed examination of the bonding around Br in a still simpler model.

Insight from a Model BrH_4^{3+} System

In order to study the geometry around the Br atom, a simple model, BrH_4^{3+} was considered. Calculations were performed on this system keeping the Br-H distance constant at 2.6 Å. Initially the Br atom was kept in the plane of the H atoms. The orbital diagram is shown in Figure 2. Many of the orbital features of these molecules have been discussed by Gimarc⁴⁶ and by Minkin and co-workers.⁴⁷

$1a_{1g}$ is composed mainly of the Br s orbital while the e_u is a degenerate orbital having the p_x and p_y of Br mixing with appropriate linear combinations of H atomic orbitals. The highest occupied molecular orbital is the b_{1g} , a nonbonding orbital on Br. There is no Br orbital of b_{1g} symmetry. Similarly, the Br p_z is orthogonal to all H orbitals. Therefore, the eight electrons in the system occupy three bonding molecular orbitals and one nonbonding molecular orbital. So, in a localized picture, the molecule has only three pairs of bonding electrons to form four bonds.

When the Br atom is pulled 1.5 Å out of the plane of H atoms, the Br-H distance is still maintained at 2.6 Å. The a_{2u} containing the Br p_z orbital is now stabilized by bonding interactions and falls below the e_u set, thus making the nonbonding b_{1g} the lowest unoccupied molecular orbital. There is an effective level crossing along this seemingly minor geometrical distortion. The HOMO is stabilized by 0.9 eV compared to the planar system. Now there are four pairs of electrons occupying four bonding orbitals. The Br-H overlap population in the square planar geometry is 0.13, compared to 0.15 in the square pyramidal geometry. Note the great improvement in the HOMO-LUMO gap in the square pyramidal geometry. The square planar to square pyramidal distortion can be described as a typical second-order Jahn-Teller deformation.⁴⁸ A nonbonding molecular orbital in the square

(46) Gimarc, B. M. *Molecular Structure and Bonding: The Qualitative Molecular Orbital Approach*, Academic: New York, 1979.

(47) Minkin, V. I.; Simkin, B. Ya.; Minyaev, R. M. *Quantum Chemistry of Organic Compounds*; Springer-Verlag: Berlin, Heidelberg, Germany, 1990.

(48) Pearson, R. G. *Symmetry Rules for Chemical Reactions*, Wiley-Interscience: New York, 1976.

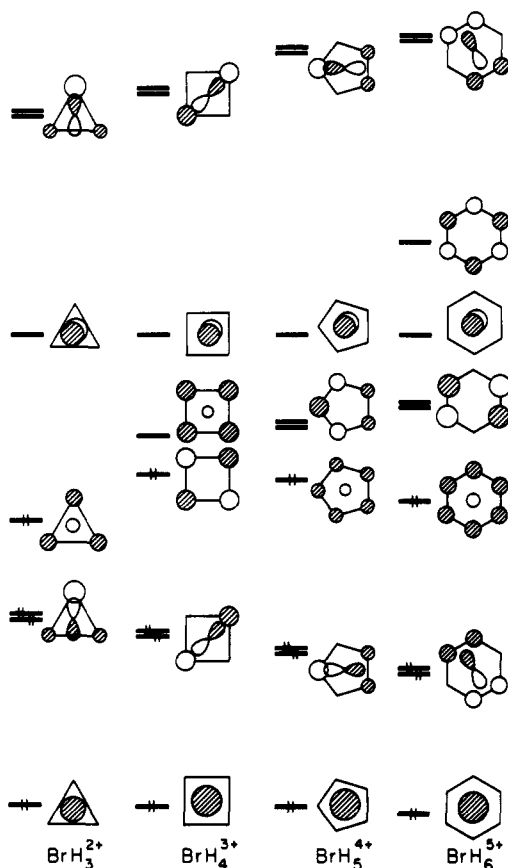


Figure 3. Molecular orbitals for planar $\text{BrH}_n^{(n-1)+}$, $n = 3, 4, 5$, and 6 .

Table III. Overlap Population of Br-H Bond in $\text{BrH}_n^{(n-1)+}$

type	overlap population of Br-H (one bond)
$\mu_3\text{-BrH}_3^{2+}$	0.136
plan $\mu_4\text{-BrH}_4^{3+}$	0.130
$\mu_5\text{-BrH}_5^{4+}$	0.100
$\mu_6\text{-BrH}_6^{5+}$	0.087
tetr $\mu_4\text{-BrH}_4^{3+}$	0.161
pyr $\mu_4\text{-BrH}_4^{3+}$	0.150

planar geometry (the p_z of Br) is transformed into a bonding one upon pyramidalization.

When the geometry around the Br atom is taken as tetrahedral (right side of Figure 2), maintaining the Br-H distance at 2.6 Å, the HOMO is the t_2 set and is very close in energy to the HOMO of the square pyramidal system.

At this juncture, it is interesting to study the molecular orbitals for the planar μ_3 , μ_4 , μ_5 , and $\mu_6\text{-BrH}_n^{(n-1)+}$ model systems. These are shown in Figure 3.

In all the planar models considered, there are a total of eight electrons. Except for $\mu_4\text{-BrH}_4^{3+}$, the highest occupied molecular orbital is slightly antibonding with respect to Br and H. In all the cases there are three bonding molecular orbitals. The overlap population for these systems as well as for the tetrahedral and square pyramidal μ_4 systems is shown in Table III.

The overlap population is a maximum for the tetrahedral μ_4 case. Similar to observations for the model systems 13, 15, 17, and 18, the overlap population decreases with an increase in the number of atoms bonded to Br. So there is saturation, but it sets in slowly. The overlap population of pyramidal μ_4 lies between that of the planar and tetrahedral models.

The increased Br-H overlap population of the HOMO is an important factor for Br atom preferring a nonplanar geometry. However, it gives us no clue as to why a square pyramidal geometry is preferred over a tetrahedral one.

A more detailed analysis of the nature of orbitals indicated that, upon pyramidalization of each of the systems, one a_1 orbital is

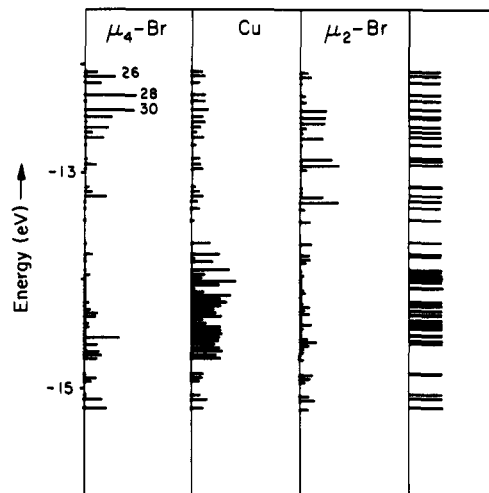
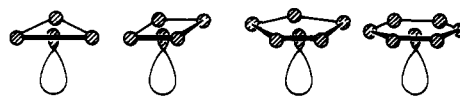


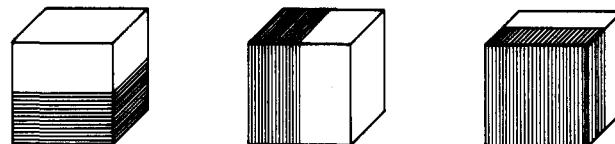
Figure 4. Projection of orbital contribution of $\mu_4\text{-Br}$, Cu, and $\mu_2\text{-Br}$ atoms to the molecular orbitals of the discrete system $\text{Cu}_6\text{Br}_3^{3-}$.

strongly stabilized and the degenerate e set is destabilized. The final shape of the critical a_1 orbital is shown in 19. Mixing in



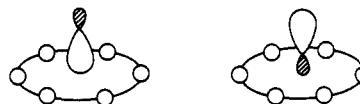
19

of s character to form a lone pair pointing away from the ligands is clearly a stabilizing feature for this orbital as is the p_z bonding with the hydrogens, which is turned on when the Br moves out of the plane. Another way to describe this orbital is it is the third p -type "united atom" orbital of an XH_n system, 20, the other ones being the e set.



20

Still another way to describe the presence of four bonding or nonbonding orbitals in XH_n systems is to invoke multicenter bonding, an extrapolation of the three-center bonding concept exploited so fruitfully by Lipscomb for boron hydrides.⁴⁹ If one forms sp hybrids along the C_n axis at the Br, one can form one bonding combination (21) and one lone pair (22), as discussed



21

22

above. The two unhybridized p_{xy} orbitals then form multicenter bonds with an appropriate symmetry-adapted ligand combination (23) of e -type symmetry. There is a total of four bonding or nonbonding orbitals.



23

The Square Pyramidal Molecular System: $\text{Cu}_6\text{Br}_3^{3-}$

A central feature of the pyramidal $\mu_n\text{-BrH}_n$ model systems of the previous section is the existence of a well-defined lone pair. It becomes interesting to see if this orbital feature is to be found

(49) Lipscomb, W. N. *Boron Hydrides*, Benjamin; New York, 1963.

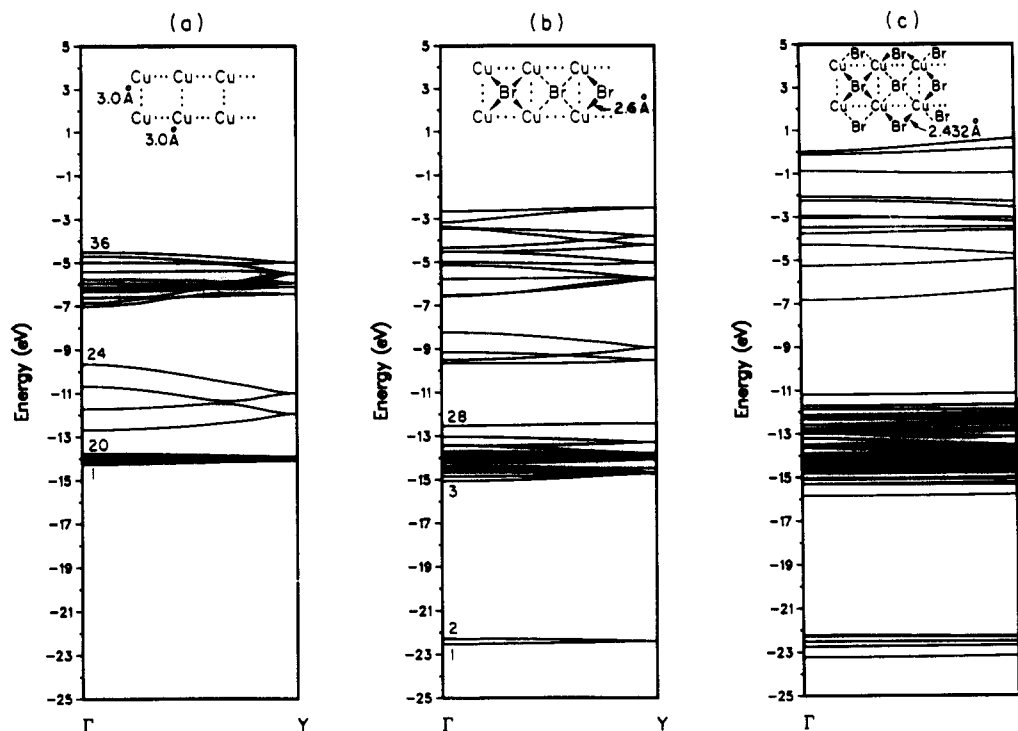
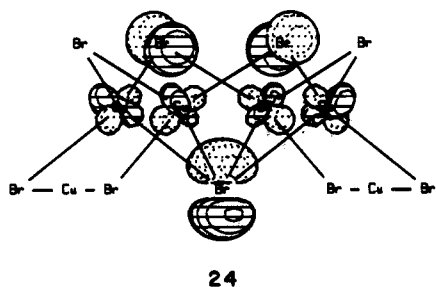


Figure 5. Calculated band structures for (a) the Cu sublattice, (b) the sublattice containing the Cu atoms and the μ_4 -Br atoms, and (c) the complete lattice.

from a calculation on an actual pyramidal μ_4 -Br containing molecule such as $\text{Cu}_6\text{Br}_9^{3-}$ shown in 6. Calculations on this molecule gave a band of Br 4s levels at -22.0 eV and Cu 3d levels around -14.0 eV. The bonding and nonbonding Br 4p levels mix with Cu 3d and 4s in the region between -12.0 and -15.0 eV. The orbital energies are shown in Figure 4. This is analogous to the projection of density of states for extended systems.³⁸ The horizontal length of a "stick" measures the contribution of the specified atom to the composition of each molecular orbital. The first column shows the projection of molecular orbitals having a μ_4 -Br contribution. The second column shows the contribution of one of the Cu atoms, and the third corresponds to μ_2 -Br contribution. Though many levels are very close in energy and may even be degenerate, they have been shown as individual "sticks" in the first three columns of the figure. In order to get a feeling for the energy level distribution in the energy range -16.0 to -12.0 eV, the levels are marked on the extreme right of the figure at appropriate energy values. Atomic orbitals of μ_4 -Br atoms are distributed over numerous molecular orbitals. The biggest μ_4 -Br concentrations close to the HOMO are in the orbitals marked 26, 28, and 30. Further analysis of these three molecular orbitals showed that while molecular orbitals 26 and 28 have p_x and p_y contributions, molecular orbital 30 contains p_z of μ_4 -Br. This orbital is of interest to us since our intention is to find a molecular orbital with the lone pair character on μ_4 -Br. A representation⁵⁰ of orbital 30 is shown in 24. While the Cu contributions in this molecular orbital are small, it has substantial μ_2 -Br character mixed in.



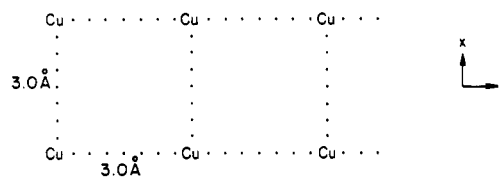
24

We proceed next to the band structure of the extended polymer 10.

The One-Dimensional Polymer: Cu_2Br_3^-

In order to understand the bonding in the extended structure 10, we have averaged the bond lengths of all the chemically equivalent bonds. In the real system the Cu...Cu distances are 2.86 Å along the chain direction and 3.09 Å perpendicular to the chain direction. We have considered an idealized system with all the Cu...Cu distances equal to 3.0 Å. The μ_4 -Br-Cu distance is 2.6 Å and the μ_2 -Br-Cu distance is 2.432 Å. The basic unit cell is made up of Cu_2Br_3^- units. Initially we look at the Cu sublattice and then we study the interaction of the μ_4 -Br with Cu by introducing the Br atoms in the center. Finally, we include the μ_2 -Br atoms in the lattice.

To facilitate the subsequent comparison with the complete system, which has a glide plane of symmetry, we have considered four Cu atoms in a unit cell as shown below. The chain extends along the y -direction, as indicated in 25. The band structure of



25

this chain is seen in Figure 5a. The group of 20 bands located at -14.0 eV consists of Cu d-bands, which show little dispersion. Bands 21–24 are the in-phase and out-of-phase linear combinations of Cu s-orbitals. Bands 25–36 are due to the p-orbitals. The total overlap population is 0.02 for Cu...Cu perpendicular to the chain and is the same along the chain.

Proceeding to the one-dimensional chain with the inclusion of the μ_4 -Br, we have maintained all the μ_4 -Br-Cu distances at 2.6 Å. Since the Br p-orbitals are close in energy to the Cu d-orbitals, there is some interaction between them. The band structure is shown in Figure 5b for $\text{Cu}_4\text{Br}_2^{2+}$ chain. Here, only the μ_4 -Br atoms have been introduced in the lattice. The bands in the region -7.0 to -2.0 eV are combinations of Cu p-orbitals and Br p-orbitals.

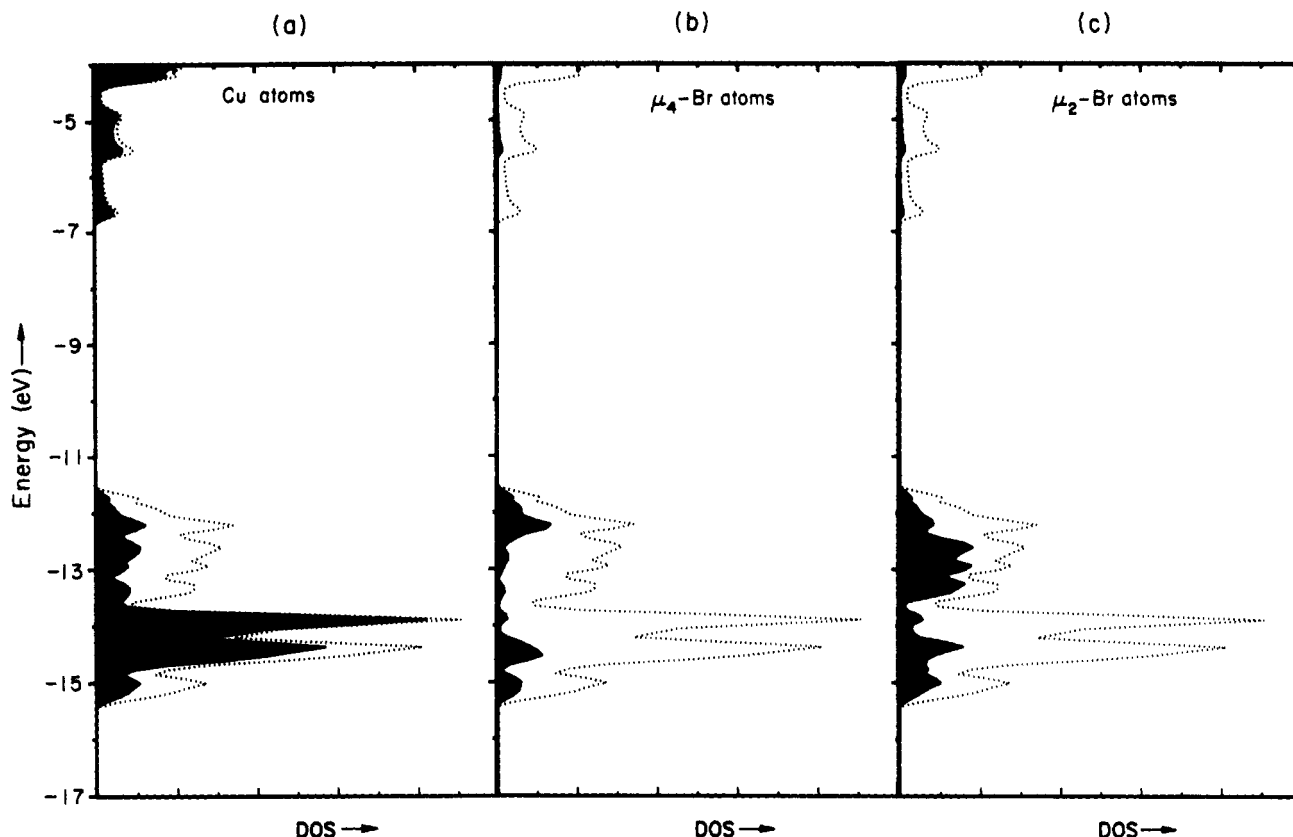


Figure 6. Calculated DOS for the $(\text{Cu}_2\text{Br}_3)_n$ polymeric system. The projections (shaded areas) indicate the contributions to this DOS from (a) Cu atoms, (b) μ_4 -Br atoms, and (c) μ_2 -Br atoms.

Bands 26–28 are localized largely on Br p-orbitals with a small contribution from Cu d-orbitals. Bands 1 and 2 correspond to Br s-orbitals. Bands 3–8 are combinations of Cu s and Br p-orbitals while bands 9–22 are mainly Cu d-orbitals. At Γ , band 29 of Figure 5b is similar to band 24 of Figure 5a, since there is no Br contribution to this band. Bands 30–32 have all increased in energy at Γ compared to the respective bands 21–23 in Figure 5a because of antibonding interactions of Br p-orbitals with Cu s-orbitals. The total overlap population between Cu and Br is 0.26, for the Cu–Cu interactions perpendicular to the chain it is 0.01, and that along the chain is 0.03. The observed bond length in the real system is 3.09 Å perpendicular to the chain and 2.86 Å along the chain direction. This trend seems to be reflected in the total overlap populations, though these are small.

The μ_2 -Br atoms were introduced next, with the band structure shown in Figure 5c, and the bonding in the system was studied with the help of decompositions of densities of states (DOS) and crystal orbital overlap populations (COOP). Figure 6 shows the DOS of Cu, μ_4 -Br, and μ_2 -Br. It is rather difficult to identify any crystal orbital or band as the μ_4 -Br lone pair, though there is a peak in the μ_4 -Br contribution around -12.0 eV.

The COOP curves for the various Br–Cu interactions are shown in Figure 7. Just below the Fermi level (which is at -11.7 eV), both of the Br–Cu interactions are antibonding. However, the total overlap population is bonding in all cases. Around the region of -12.0 eV, the μ_4 -Br–Cu interaction is slightly antibonding and might be considered to be similar to the molecular orbital 30 shown in structure 24 for the discrete molecule. From the DOS projections (for single atoms), the orbitals around this energy value were found to have a greater contribution from each μ_4 -Br atom (about 20%) than from each Cu atom (about 4%). Further breakdown of the projection of DOS in terms of orbitals indicated that, around this region, there is greater contribution from the p_z orbital of μ_4 -Br than from other orbitals. Magnified projections of p_x , p_y , and p_z orbitals of μ_4 -Br along with the total density of states is shown in Figure 8.

The crystal orbital overlap population is 0.20 for μ_4 -Br–Cu and 0.35 for μ_2 -Br–Cu. The total overlap for μ_2 -Br–Cu is larger than

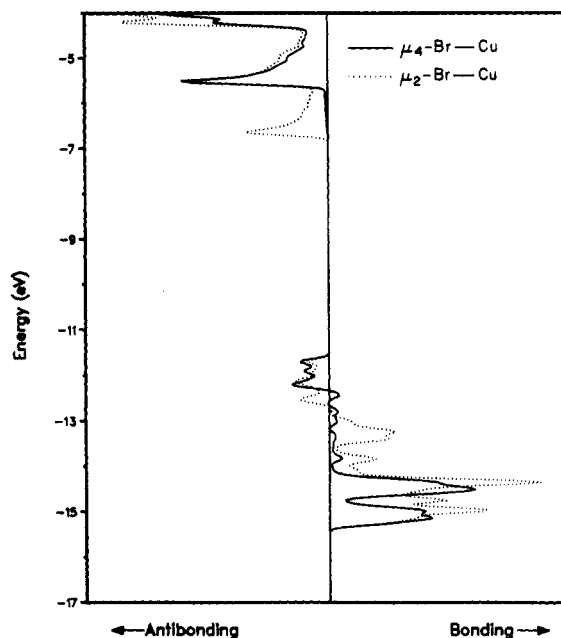


Figure 7. Crystal orbital overlap population (COOP) curves for μ_4 -Br–Cu (solid line) and μ_2 -Br–Cu (dotted line).

that for μ_4 -Br–Cu, and in order to compare their bond strengths, the calculation was repeated on the polymeric chain while keeping all the Br–Cu distances equal to 2.6 Å. The crystal orbital overlap population is 0.22 for μ_4 -Br–Cu and 0.25 for μ_2 -Br–Cu. Here again the overlap population is larger for μ_2 -Br–Cu than for μ_4 -Br–Cu, though the difference is not as large as in the previous calculation.

Tetrahedral versus Square Pyramidal μ_4 -Br

One possible alternative structure for a polymeric chain with the same stoichiometry (Cu_2Br_3^-) where the μ_4 -Br is tetrahedral

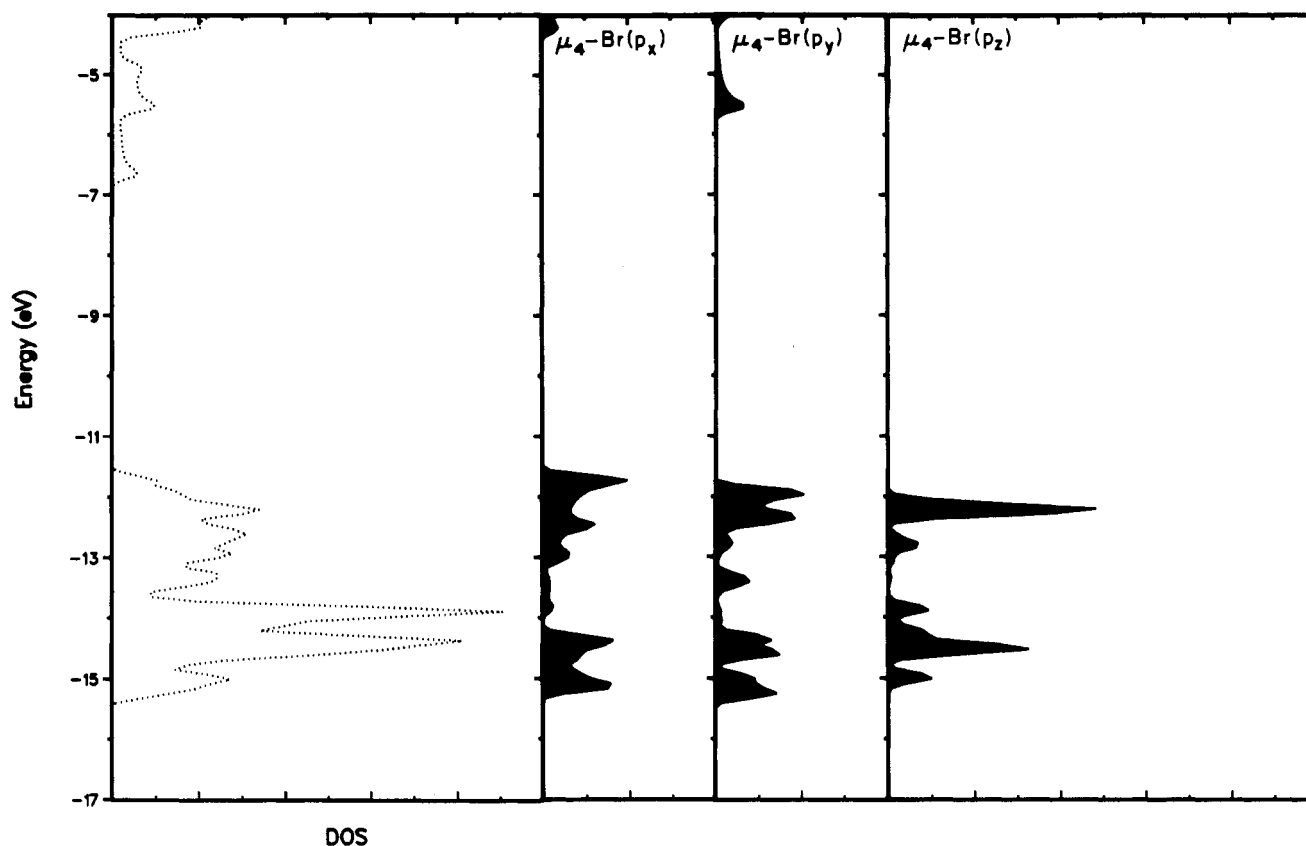
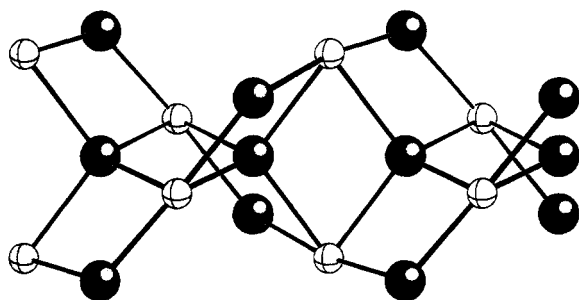


Figure 8. Calculated DOS for the $(\text{Cu}_2\text{Br}_3)_n$ polymeric system. The magnified projections (shaded areas) indicate the contributions to this DOS from p_x , p_y , and p_z atomic orbitals of μ_4 -Br atoms.

is **26**. Here the large dark circles denote Br atom while the smaller circles represent Cu atoms.



26

In an attempt to construct a geometry similar to the one-dimensional chain **10**, here the μ_4 -Br-Cu distance is maintained at 2.6 Å while the μ_2 -Br-Cu distance is 2.43 Å. Calculations revealed that this structure was destabilized by about 10.0 eV compared to the corresponding one with a pyramidal μ_4 -Br!

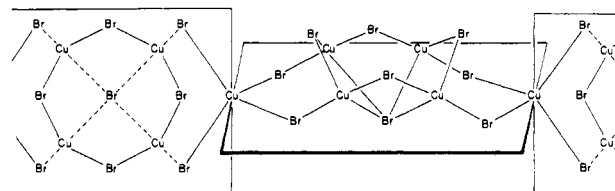
Why is this system so unstable? The total DOS, magnified projection of the orbitals of tetrahedral μ_4 -Br, and the COOP curves are shown in Figure 9 for this hypothetical polymeric chain. The Fermi level falls at -8.46 eV for this system as compared to -11.71 eV for system **10**. Comparing the COOP curves in Figures 7 and 9, it can be seen that the μ_4 -Br-Cu interaction is antibonding in the region -12.5 to -14.0 eV in the latter while it is bonding in the former. The COOP for μ_2 -Br-Cu is 0.36 while that of the tetrahedral μ_4 -Br-Cu is 0.10. These values are to be compared with the COOP of 0.20 obtained for the pyramidal μ_4 -Br-Cu and 0.35 for the μ_2 -Br-Cu for the real system, **10**. In the tetrahedral system, **26**, there is a great decrease in μ_4 -Br-Cu bonding interactions and a slight increase in Br...Br and Cu...Cu antibonding interactions.

It is clear that this hypothetical structure, constructed in an attempt to find a polymer with a tetrahedral μ_4 -Br, is under much strain. The coordination at each Cu is highly distorted, and the

set of six angles around Cu is 64.7, 106.5, 70.5, 170.0, 106.5, and 64.7, clearly very far away from either tetrahedral or square planar. We think the problem is at the copper, not the bromide. But it is hard to think of an unstrained tetrahedral Br chain with the same stoichiometry.

Hypothetical Structures

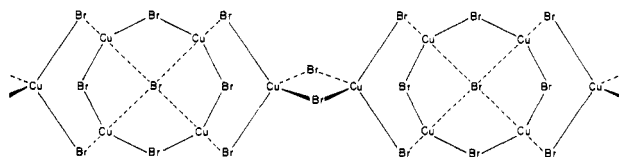
It would be nice to keep ahead of the richness that nature offers to us even within this limited realm of copper halide polymers. So we have begun to think of some hypothetical structures based on the heretofore observed geometrical features in halocuprates. Our first idea was to try to extend the structure shown for the discrete molecule **6**. Keeping the μ_4 -Br at the apex of a square pyramid and maintaining tetrahedral coordination around all the Cu atoms, one comes to **27**. Since all Cu atoms are assumed to



27

be tetrahedral, if the first unit of $\text{Cu}_5\text{Br}_9^{4-}$ is in one plane the next unit will be in a plane perpendicular to the first.

Alternately, we could bridge two monomer units with two Br atoms as shown in **28**. The stoichiometry is $\text{Cu}_6\text{Br}_{11}^{5-}$.



28

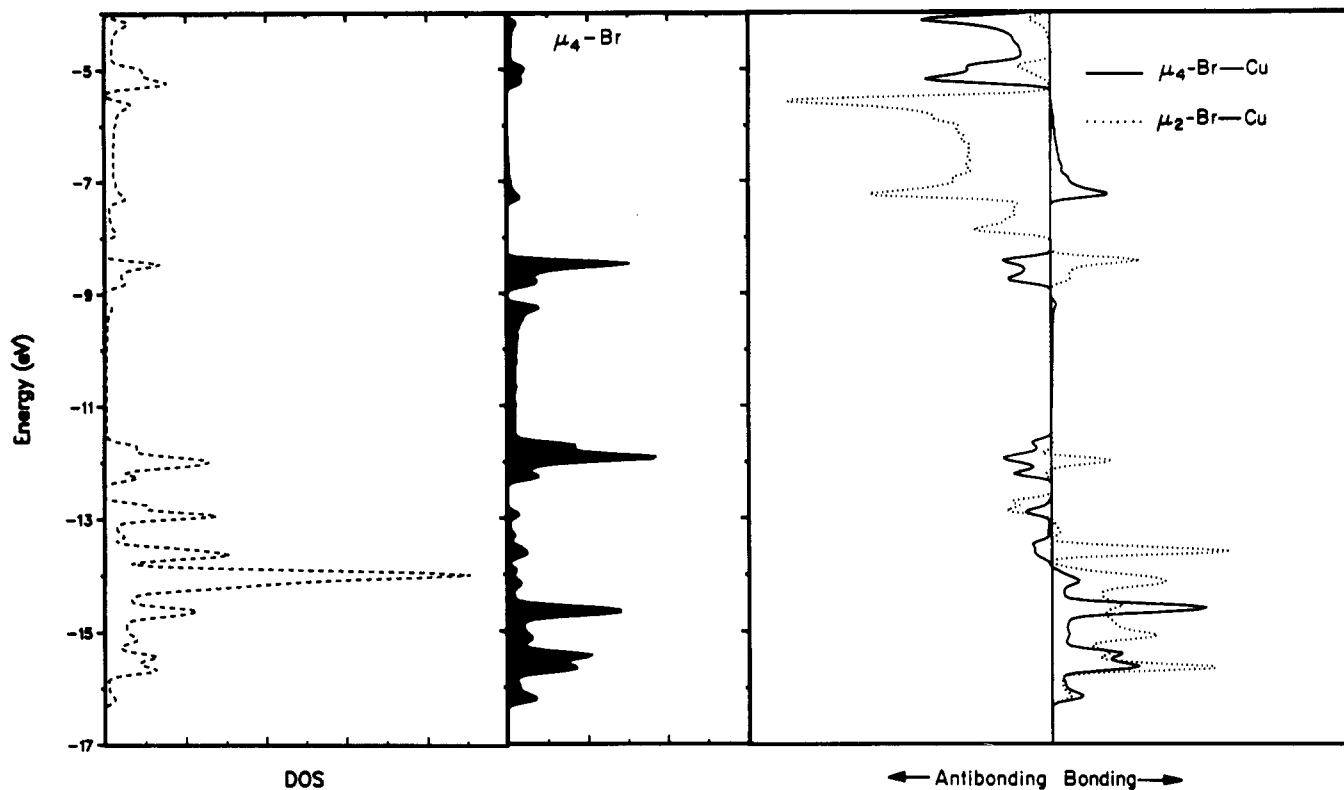


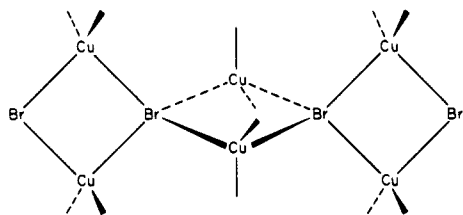
Figure 9. First panel: calculated total DOS for the hypothetical polymer with tetrahedral geometry around μ_4 -Br. Second panel: magnified projection of μ_4 -Br atoms. Third panel: COOP plot for the Br-Cu interactions. The μ_4 -Br-Cu interaction is represented by a solid line, and μ_2 -Br-Cu, by a dotted line.

Table IV. Extended Hückel Parameters

atom	orbital	H_{ij} , eV	slater exponent ζ^a	ref
Cu	3d	-14.00	5.95 (0.5935), 2.30 (0.5742)	51
	4s	-11.40	2.20	
	4p	-6.06	2.20	
Br	4s	-22.07	2.59	52
	4p	-13.10	2.13	

^a Exponents and coefficients (in parentheses) in a double- ζ expansion of the metal d-orbitals.

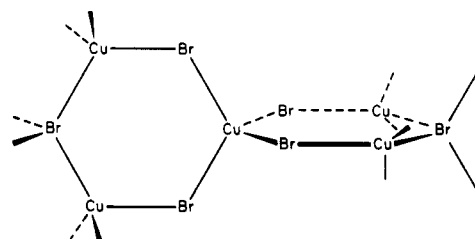
Further possibilities can be imagined for a one-dimensional structure involving a tetrahedral μ_4 -Br. One simple way this may occur is shown in 29. However, now there are terminal Br (or other ligand) atoms attached to Cu atoms.



29

Another possibility is a linear polymer with six-membered rings,

30. This is a one-dimensional piece of the zinc blende structure of extended copper halides.



30

It is highly probable that the next copper halide polymeric system made will not be one of these, but a still different one. This is the fun of chemistry.

Acknowledgment. We thank Jane Jorgensen for her excellent drawings. Our research was supported by the National Science Foundation through Research Grant CHE-8912070.

Appendix

The extended Hückel parameters used in this work are shown in Table IV.

Registry No. 4, 54854-76-1; 6, 121500-82-1.

(51) Hay, P. J.; Thibeault, J. C.; Hoffmann, R. *J. Am. Chem. Soc.* **1975**, *97*, 4884.

(52) Alvarez, S.; Mota, F.; Nova, J. *J. Am. Chem. Soc.* **1987**, *109*, 6586.